Acta Mechanica 144, 1–15 (2000)

ACTA MECHANICA

Phenomenological nonlocal approaches based on implicit gradient-enhanced damage

M. G. D. Geers, R. H. J. Peerlings and **W. A. M. Brekelmans,** Eindhoven, and
R. de Borst, Delft, The Netherlands

(Received May 31, 1999; revised November 20, 1999)

Summary. The present paper focusses on five phenomenological approaches in gradient-enhanced damage, several of which have been proposed in the literature to simulate material degradation. These different gradient-damage based nonlocal models are examined with respect to their ability to describe crack initiation and crack propagation. The models are applied to identical mechanical benchmark tests, where the material damage evolution law is taken as good as possible equal for each model. Interesting differences between the different models arise, and it is shown that care must be taken in the interpretation and application of these models. One-dimensional results cannot be extrapolated in a straightforward fashion to two dimensions, and the physical relevance of some results is in some cases debatable. Furthermore, it is shown that the response of some models is strongly influenced by small differences in the applied damage evolution law. A discussion is made on the use of two different types of such evolution laws, which are frequently applied in the literature.

1 Introduction

Significant progress has been made in the development of constitutive models which are capable to describe the damage process in a quasi-brittle material. A variety of models are nowadays available, and it is not always clear which model is best suited for real engineering problems. Nevertheless, the necessity for the use of models which rely on the principle of nonlocal action has become clear in recent years. Although often motivated by computational arguments, more and more examples become available which justify the principle of nonlocal action on a physical basis [1]–[4]. The nonlocal continuum was already introduced in the sixties to describe elastic material behaviour, see for instance Eringen [5]. Maugin [6] was one of the first to underline the importance of nonlocal theories in different fields of physics. The main argument for nonlocality resides in the fact that a perfect continuum (satisfying the principle of contiguity) does not really exist, and that at some scale each material will have a discrete character which does not permit application of the classical principle of local action (which is one of the main assumptions in classical continuum mechanics). Damage is a typical example of a physical phenomenon which takes place at the discrete level of the material, i.e. in the microstructure, or more specific at interfaces, bonds, molecular chains, etc. Hence, damage theories cannot be developed consistently without taking into account this microstructure, which justifies a nonlocal constitutive model in damage mechanics. The complexity of the physical damage process is often simplified to a high extent in nonlocal constitutive models. Most nonlocal models are limited to the addition of

one extra variable, which is commonly denoted as the intrinsic length scale of the continuum. It is not trivial to link this length parameter to all the geometrical and physical properties of the microstructure of a material, since this length scale is not solely a geometrical characteristic of the microstructure, but also depends on the mechanics of the discrete bonds in the microstructure [7]–[9]. A more thorough insight in the relation between microstructural properties and nonlocal continuum models is needed to clarify the physical backgrounds of this length scale.

Amongst the gradient-enhanced damage models, the so-called implicit gradient-enhanded models (i.e. where the nonlocality ensues from the solution of a partial differential equation) appear to be most successful, since they present all characteristics of the earlier developed nonlocal damage models while preserving the computational advantages of the gradient type models. Indeed, it has been shown that these implicit gradient-damage formulations can be easily recast in an integral form, which is characteristic for the nonlocal damage approach [10]. Furthermore, the Neumann boundary condition which is commonly used to solve the partial differential equation (of the Helmholtz type) for the nonlocal variable automatically involves larger nonlocal weight factors for the material close to the boundaries of the considered continuum [10]. This is particularly advantageous from a physical point of view, since the model will then be more sensitive to surface defects compared to classical nonlocal damage models.

A comparison of some (integral) nonlocal models for damage and fracture has been perfomed by Jirásek [11], for uniaxial tension. It was shown that some of the analyzed formulations inevitably lead to residual stresses and that they are not capable of modeling a complete macroscopic crack. This paper concerns different types of damage formulations, which are all casted in the implicit gradient form. Various choices and possibilities have been proposed in the literature, where separate examples with different materials were used for each model. An in-depth comparison has not been performed, and the consequence of the use of one model or another is not clear. Using identical examples and nearby similar damage evolution laws, this paper reveals hidden properties of the proposed models and clarifies the influence of various choices in gradient damage modelling. The analysed benchmark examples permit to investigate crack initiation and crack propagation, in a one-dimensional and two-dimensional context. Variable or so-called transient length scales [7], [12] have been introduced in some of the models to investigaste the influence on the mechanical behaviour during the fracture process. The comparison is made for an isotropic quasi-brittle elasticity-based damage formulation. The description of each model is limited to the essence which is necessary to understand the sequel of the paper. The detailed numerical implementation of some models has been elaborated in the literature [12]–[15], while the numerical scheme for the other models can be easily derived on the basis of the similitude between the applied Helmholtz partial differential equations. Practical applications have been reported for some models [8], [9], [16], [17]. It is emphasized that all the presented models correctly regularize the energy dissipation.

2 Phenomenological approaches in implicit gradient-enhanced damage

The spatially nonlocal concept has been embedded in various ways into damage models. The nonlocal character or gradient enhancement can be applied to different types of variables: an equivalent strain measure [12], [13], a history parameter [14], [18], or the damage variable [4],

[19], [20]. Furthermore, formulations exist in which the intrinsic length scale is treated as a constant [13] or alternatively as a variable [8], [12]. Since implicit gradient formulations are best suited for numerical analyses, attention will next be given to five implicit gradient-enhanced damage formulations which are based on a nonlocal equivalent strain $\bar{\varepsilon}_{eq}$, a nonlocal history parameter $\bar{\varkappa}$ and a nonlocal damage variable $\bar{D}$. Two of the considered models have a constant length scale while the three remaining models introduce a variable character to the length parameter.

All formulations are developed within an isotropic strain-based damage mechanics framework. The classical total stress-strain relation then reads

$$\boldsymbol{\sigma} = (1 - D)\,{}^4\boldsymbol{C} : \boldsymbol{\varepsilon}\,. \tag{1}$$

Herein, $\boldsymbol{\sigma}$ represents the Cauchy stress tensor, $\boldsymbol{\varepsilon}$ the infinitesimal strain tensor and ${}^4\boldsymbol{C}$ the fourth-order elastic stiffness tensor. The damage is denoted by a scalar-valued variable D, which satisfies the constraint

$$0 \leq D \leq 1\,. \tag{2}$$

In the local damage mechanics concept, the influence of the current deformation state on the damage is quantified by a local equivalent strain ε_{eq}, which is a scalar function of the different components of the strain tensor. The equivalent strain is used to map the tensorial strain state to a scalar-valued variable which can be used to drive the damage growth. This permits to give a triaxial character or a compression-tensile sensitivity to the damage growth. The scalar definition of ε_{eq} may take various forms, depending on the material considered. For an overview of some definitions, see [16]. Here, the normalized energy release rate is used to compare the different models:

$$\varepsilon_{eq}(\boldsymbol{\varepsilon}) = \sqrt{\frac{\boldsymbol{\varepsilon} : {}^4\boldsymbol{C} : \boldsymbol{\varepsilon}}{E}}\,. \tag{3}$$

The damage D is then coupled to the loading history through a monotonically increasing deformation history parameter $\varkappa$ that equals the maximum value of ε_{eq} throughout the entire loading history. The damage evolution is then fully described by the scalar function $D(\varkappa)$. The relation between the history parameter $\varkappa$ and the equivalent strain ε_{eq} is given by the Kuhn-Tucker loading-unloading relations

$$\dot{\varkappa} \geq 0\,, \qquad \varepsilon_{eq} - \varkappa \leq 0\,, \qquad \dot{\varkappa}(\varepsilon_{eq} - \varkappa) = 0\,. \tag{4}$$

The nonlocal character is generally implemented in the damage evolution. However, this can be realized in various ways. Each approach starts from a local variable ϕ which is transformed into a nonlocal variable $\bar{\phi}$ by means of a Helmholtz-type partial differential equation,

$$\bar{\phi} - c\nabla^2\bar{\phi} = \phi\,, \tag{5}$$

where c is a positive scalar, related to the square of the length parameter. Such a differential form can be derived from the nonlocal integral form through a Taylor series expansion, see [13], [21]. The partial differential equation (5) is complemented with the following Neumann boundary condition on the boundary Γ:

$$\vec{\nabla}\bar{\phi} \cdot \vec{n} = 0\,. \tag{6}$$

In the following subsections, five different approaches to embed a nonlocal character into the damage formulation, based on Eq. (5), will be analyzed.

2.1 Nonlocal equivalent strain model

The most used choice in nonlocal damage mechanics is to adopt $\phi = \varepsilon_{eq}$, which leads to the use of a nonlocal equivalent strain $\bar{\varepsilon}_{eq}$. Equation (5) is then transformed into

$$\bar{\varepsilon}_{eq} - c\nabla^2\bar{\varepsilon}_{eq} = \varepsilon_{eq}\,, \tag{7}$$

with the boundary condition

$$\vec{\nabla}\bar{\varepsilon}_{eq}\cdot\vec{n} = 0 \tag{8}$$

on Γ. Note, that the intrinsic length scale $\ell_c = \sqrt{c}$ is here treated as a constant. The damage D is computed from the history parameter $\varkappa$, which is now determined by

$$\dot{\varkappa} \geq 0\,, \qquad \bar{\varepsilon}_{eq} - \varkappa \leq 0\,, \qquad \dot{\varkappa}(\bar{\varepsilon}_{eq} - \varkappa) = 0\,. \tag{9}$$

Computational details and numerical results for this model can be found in [13].

2.2 Nonlocal history parameter model

A second choice is to take the local history parameter determined from (4) as the source term for (5), i.e. $\phi = \varkappa$, see [14], [18]

$$\bar{\varkappa} - c\nabla^2\bar{\varkappa} = \varkappa\,, \tag{10}$$

with the Neumann boundary condition

$$\vec{\nabla}\bar{\varkappa}\cdot\vec{n} = 0\,. \tag{11}$$

Since Eq. (10) can be rewritten in the nonlocal integral form, it is clear that $\bar{\varkappa}$ will preserve the monotonically increasing character of $\varkappa$. This ensures that the damage D never decreases, as required by the Clausius-Duhem inequality.

2.3 Nonlocal damage model with a transient length scale

Inspired by Frémond and Nedjar [20], and de Borst et al. [14], the nonlocal variable can also be derived from the damage, i.e. $\phi = D$. This suggestion was also made by Bažant and Pijaudier-Cabot [19]. However, Jirásek [11] already showed that such a nonlocal model cannot provide meaningful results with a constant length parameter. A partial differential equation (5) with a variable length scale is therefore used instead

$$\bar{D} - c(D)\nabla^2\bar{D} = D\,, \tag{12}$$

while the boundary condition on Γ is given by

$$\vec{\nabla}\bar{D}\cdot\vec{n} = 0\,. \tag{13}$$

The nonlocal damage variable is then used in the constitutive relationship

$$\boldsymbol{\sigma} = (1-\bar{D})\,{}^4\boldsymbol{C} : \boldsymbol{\varepsilon}\,. \tag{14}$$

The latter relation shows that it is no longer possible to keep the gradient parameter $c = \ell_c{}^2$ constant. If this would be the case, the nonlocal damage $\bar{D}$ which enters Eq. (14) will never

reach the ultimate point of failure ($\bar{D} = 1$) since the local damage D is bounded by the relations (2), see also [11]. Accordingly, a nonlocal damage model in this sense can only be realistic if $\bar{D}$ approaches unity when its local counterpart D does so. The gradient parameter must therefore depend on the local damage variable D. If the local damage equals unity, the intrinsic length scale will equal zero, and the nonlocal and local damage variables will then coincide. Since the gradient term vanishes only after the crack is fully initiated, the well-posedness remains preserved during the initiation phase. In the present analysis, the gradient parameter c decreases linearly with the damage D, according to the following relationship:

$$c(D) = (1 - D)\, c_{\max} . \tag{15}$$

2.4 Nonlocal equivalent strain model with a damage-dependent transient length scale

If the nonlocal equivalent strain model (7) is combined with the transient character for the gradient parameter adopted in Eq. (12), the following formulation is obtained:

$$\bar{\varepsilon}_{eq} - c(D)\, \nabla^2 \bar{\varepsilon}_{eq} = \varepsilon_{eq} . \tag{16}$$

This equation is solved in conjunction with Eqs. (8) and (9). The length scale diminishes with the increase of damage, as described by relation (15). Once damage is fully developed, the model again coincides with the local model, since then $\bar{\varepsilon}_{eq} = \varepsilon_{eq}$.

2.5 Nonlocal equivalent strain model with a strain-dependent transient length scale

A strain-based transient gradient-damage model (or nonlocal equivalent strain model) has been proposed in [12] and has been successfully applied to composite materials [8], [9]. The analysis of damage in discrete models with respect to the consequences on continuum models has shown that the internal length scale of a continuum increases with the damage of the system [7]. This observation is in agreement with the transient nature adopted in [12], where the gradient parameter increases with the local equivalent strain ε_{eq}. It has also been shown that the transient character of the length scale alleviates spurious damage development with the use of exponential damage evolution laws [12]. The transient character of the intrinsic length scale in this case is thus opposite to the two previous models, where the length scale decreased with increasing damage. The equation to solve is rewritten as

$$\bar{\varepsilon}_{eq} - c(\varepsilon_{eq})\, \nabla^2 \bar{\varepsilon}_{eq} = \varepsilon_{eq} , \tag{17}$$

while the boundary condition (8) is applied. The gradient parameter increases linearly with ε_{eq}, which means that the nonlocal interaction becomes more important for increasing local strains.

For the considered model material in the next section, the transient evolution of c is described by the following bilinear relationship:

$$c(\varepsilon_{eq}) = \begin{cases} c_{\max} \dfrac{\varepsilon_{eq}}{\epsilon_{\max}} & \text{if } \varepsilon_{eq} \leq \epsilon_{\max} \\ c_{\max} & \text{if } \varepsilon_{eq} > \epsilon_{\max} , \end{cases} \tag{18}$$

where $\epsilon_{\max}$ is the equivalent strain level at which the maximum length scale $\sqrt{c_{\max}}$ is reached.

3 Damage evolution law

It is known from the literature that the adopted damage evolution law $D(\kappa)$ or $D(\bar{\kappa})$ is an important charateristic to describe the global mechanical response, especially after the ultimate load has been reached, i.e. the post-peak behavior. Here, two damage evolution laws will be used, a power-law and an exponential softening law. Both evolution laws match well in the initial post-peak regime but exhibit some small differences in the final failure stages. Damage initiates ($\dot{D} > 0$) for both cases when the history parameter κ exceeds a threshold value κ_i, which is the initial value of κ at time $t = 0$. This threshold value represents the ultimate (local or nonlocal) equivalent strain or nonlocal history parameter that characterizes the elastic material behavior prior to the occurrence of damage. The power-law damage evolution law used in the analysis is given by

$$D = 1 - \frac{\kappa_i}{\kappa} \left(\frac{\kappa_c - \kappa}{\kappa_c - \kappa_i} \right)^{\alpha}, \tag{19}$$

where the ultimate damage level ($D = 1$) is reached for a finite value of the history parameter κ_c. The parameter α is the decay parameter. In the exponential law, on the other hand, the damage variable approaches unity but the limit value $D = 1$ is never reached,

$$D = 1 - \frac{\kappa_i}{\kappa} e^{[-\beta(\kappa - \kappa_i)]}. \tag{20}$$

This type of evolution law induces a long tail in the stress-strain softening curve. The exponential development of damage is described by the material parameter β. The material which will be examined using the different damage models in the subsequent Sections is characterized by a Young's modulus of 10 000 MPa, a Poisson's ratio equal to 0.3, a damage initiation threshold $\kappa_i = 0.001$ and a gradient parameter $c = 5$ mm^2. The transient evolution of c for the models presented in the Subsects. 2.3 and 2.5 is characterized by a maximum gradient parameter $c_{\max}$ that equals 5 mm^2, and the corresponding equivalent strain level $\epsilon_{\max}$ is 0.01. The power-law damage evolution is used with a critical value $\kappa_c = 0.05$ and a decay parameter $\alpha = 5$. The exponential law which fits closest to this power-law is obtained with $\beta = 109.525$. Both evolution laws are depicted in Fig. 1 and 2. Figure 1 shows the relation D versus κ, while Fig. 2 shows the associated stress-strain paths in the one-dimensional, homogeneous case. Figure 1 highlights that both evolution laws are very close. The corresponding responses for a uniform damaging bar are depicted in Fig. 2.

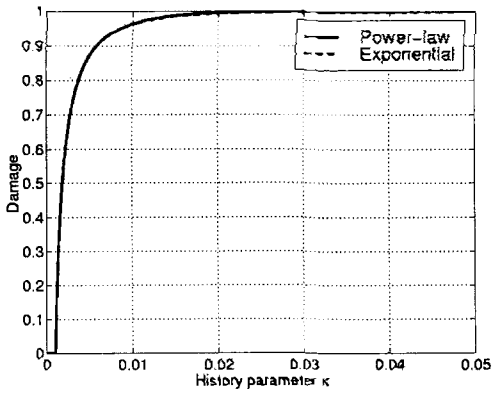

Fig. 1. Damage evolution D versus κ

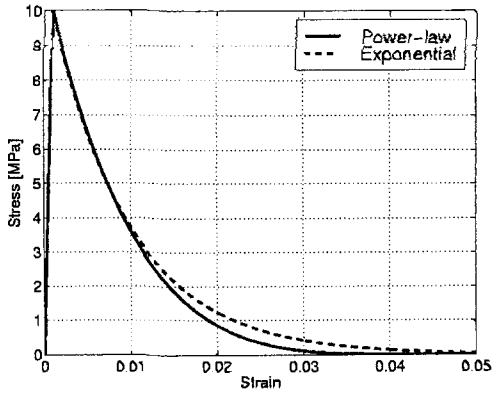

Fig. 2. Softening behavior

4 Damage and crack initiation

Damage initiation properties can be examined efficiently with a classical one-dimensional bar with a central imperfection. To this purpose a bar with a length of 100 mm and a cross-section A of 10 mm^2 is analyzed. The bar is weakened over a length of 2.5 mm at the centre by a reduction of A by 10%. One end of the bar is fixed and the other end is loaded with an axial force in tension. A similar one-dimensional analysis has been performed by Peerlings et al. [13] for Eq. (7) and by Geers et al. [12] for the damage model based on Eq. (17).

A first comparison is made between the $\bar{\varepsilon}_{eq}$ (7) and the $\bar{\kappa}$ (10) formulations. The results are shown in Fig. 3. This figure shows the force-displacement curves that ensue from the mechanical response of the bar. The main difference between these two models originates from the fact that $\bar{\varepsilon}_{eq}$ increases in loading and decreases in unloading material, while $\bar{\kappa}$ never decreases. The exponential damage evolution laws yield almost identical results, which is not the case for the power-law damage evolution. The final crack opening upon complete failure (which equals the final displacement of the bar end) differs for both cases. This difference becomes more apparent if the comparison is made for different values of α in Eq. (19). It can be noticed from Fig. 4, where the response of the $\bar{\varepsilon}_{eq}$ (7) model is shown, that the final crack opening of the bar is independent of the value of α. In this case, the local equivalent strain approaches a Dirac delta function $w\delta(x)$, where w equals the crack opening upon complete rupture of the bar. The analytical solution of Eq. (7) is easily found for a homogeneous bar with an infinite length and equals the product of w with the Greens's function associated with the Helmholtz equation (7),

$$\bar{\varepsilon}_{eq} = \frac{w\, e^{-|x|/\sqrt{c}}}{2\sqrt{c}}\,, \tag{21}$$

with $|x|$ the axial distance measured from the centre of the crack. This relation is a very good approximation for bars with finite lengths if the damaging zone is far enough from the boundaries (e.g., ten times the internal length scale). The final crack opening w_f at $x = 0$ is obtained from (21) by setting $\bar{\varepsilon}_{eq} = \kappa_c$ and solely depends on the gradient parameter c and the critical history parameter κ_c,

$$w_f = 2\kappa_c\sqrt{c}\,. \tag{22}$$

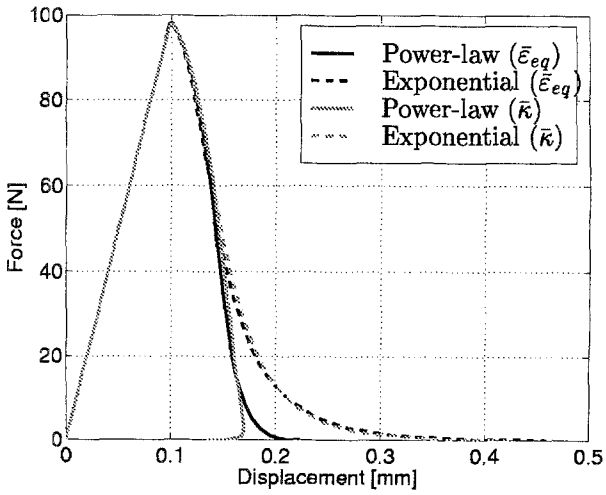

Fig. 3. Softening curves for $\bar{\varepsilon}_{eq}$ and $\bar{\kappa}$

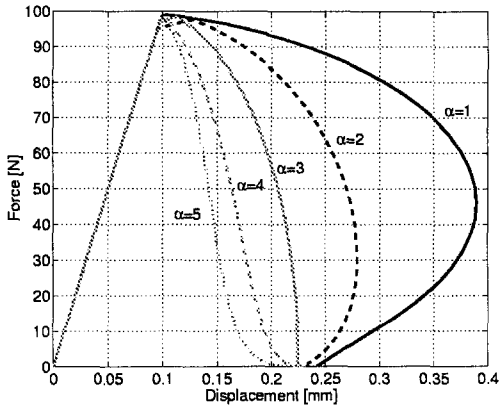

Fig. 4. Nonlocal $\bar{\varepsilon}_{eq}$-approach

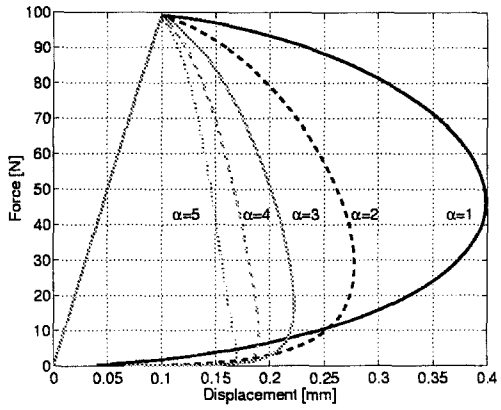

Fig. 5. Nonlocal $\bar{\kappa}$-approach

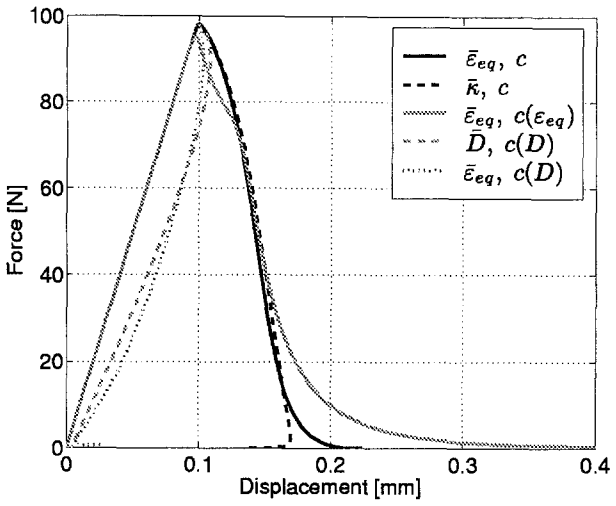

Fig. 6. Power-law softening responses

For the applied gradient parameter $c = 5$ mm^2 and the critical history parameter $\varkappa_c = 0.05$, the theoretical final crack opening equals $w_f = 0.224$ mm, which is well approached in Fig. 4.

The final crack opening which is obtained from the $\bar{\kappa}$ (10) model, presented in Fig. 5, clearly tends towards zero for each value of α, which leads to a severe snap-back behaviour in the final loading stage. For large values of α, the snap-back occurs later. This can be easily understood, since the source term in Eq. (10) no longer equals a Dirac delta function, but the envelope of the maximum strains throughout the loading history. This means that the nonlocal history parameter $\bar{\kappa}$ may reach its critical value $\varkappa_c$ even before the discontinuity at the center of the bar arises, and hence no crack opening is observed. If all models (7), (10), (12), (16), (17) are considered and a power-law damage evolution with $\alpha = 5$ is adopted, Fig. 6 is obtained. Notice that three of the five models snap back to the origin, while the two other models have a typical snap-through behavior. It can be concluded that the $\bar{\varepsilon}_{eq}$ (7), the $\bar{\kappa}$ (10) and the $[\bar{\varepsilon}_{eq}, c(\varepsilon_{eq})]$ (17) approaches lead to similar results in the initial failure stage, but to different final crack openings in the ultimate stage. The $[\bar{\varepsilon}_{eq}, c(\varepsilon_{eq})]$ (17) model converges to a large undetermined crack opening, since the process zone (where deformations localize) keeps narrowing because of the decrease of c in the unloading material next to the final crack. The nonlocal equivalent strain approaches its limit value $\varkappa_c$ asymptotically, and the local strains

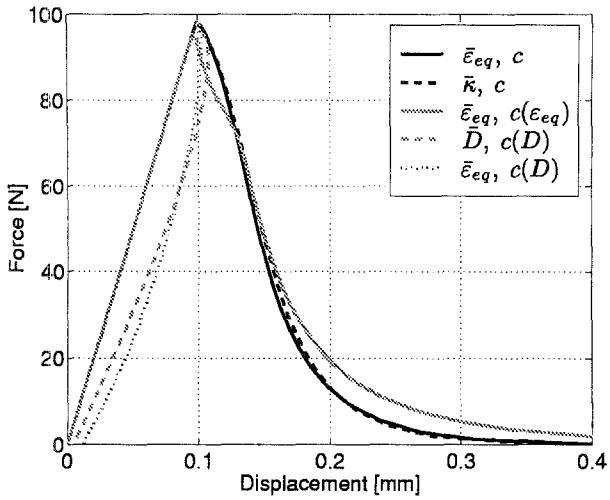

Fig. 7. Exponential softening responses

increase strongly. The two remaining transient models. $[\bar{D}, c(D)]$ (12) and $[\bar{\varepsilon}_{eq}, c(D)]$ (16) give a zero crack opening with a sharp snap-back response shortly after the initiation of damage. The zero crack opening is also the ill-posed final solution which is obtained from a local damage model. In the crack, the model converges towards a local model where D approaches unity. However, the dissipated energy now remains finite and nonzero during the entire crack initiation stage. A similar comparison can be made for the exponential damage evolution law, as depicted in Fig. 7. Notice that two of the five models snap back to the origin, while the three other models have a typical snap-through behavior. The two models with a constant length parameter and the $[\bar{\varepsilon}_{eq}, c(\varepsilon_{eq})]$ (17) model now lead to similar mechanical responses. The final crack opening for both the $\bar{\varepsilon}_{eq}$ (7) and the $\bar{\kappa}$ (10) model is now undetermined and approaches infinity. This clearly illustrates that small differences in the tail of the applied damage evolution law lead to considerable differences in the deformations of the bar. This is typically due to the fact that the crack opening (i.e., a displacement discontinuity) with an exponential law is only approximated, since the displacement jump remains smooth (theoretically there is no true crack opening at all). This seems to have a large influence on a one-dimensional bar, where the load cannot be taken over by another structural element. Indeed, the stress level is low, and in a multi-dimensional analysis the effect of this approximation is expected to vanish. For the $[\bar{D}, c(D)]$ (12) and the $[\bar{\varepsilon}_{eq}, c(D)]$ (16) models, there is almost no difference with the power-law damage evolution. At this point it is not yet clear what will be the influence of these one-dimensional results on the crack propagation. This topic is further analyzed in Sect. 5.

The final damage profiles in the bar are shown in Fig. 8 for the power-law damage evolution. It is noticed from this figure that the $[\bar{D}, c(D)]$ (12) and the $[\bar{\varepsilon}_{eq}, c(D)]$ (16) formulations both yield a sharp localized damage pattern in the bar, while the damage distribution is smoother for the three other models. The two models with a constant c have a wider damage band, which is most pronounced for the $\bar{\kappa}$ approach. This is not surprising, since the source term in Eq. (10) will always supersede the source term in (7), and thus the nonlocal variable used to compute the irreversible damage will always be larger with $\bar{\kappa}$ compared to $\bar{\varepsilon}_{eq}$. The fact that the damage is confined to a smaller region for the $[\bar{\varepsilon}_{eq}, c(\varepsilon_{eq})]$ (17) formulation stems from the fact that the length parameter is zero in the unloaded state, which leads to a smaller averaged nonlocal effect compared to the constant c models. Furthermore, the process zone

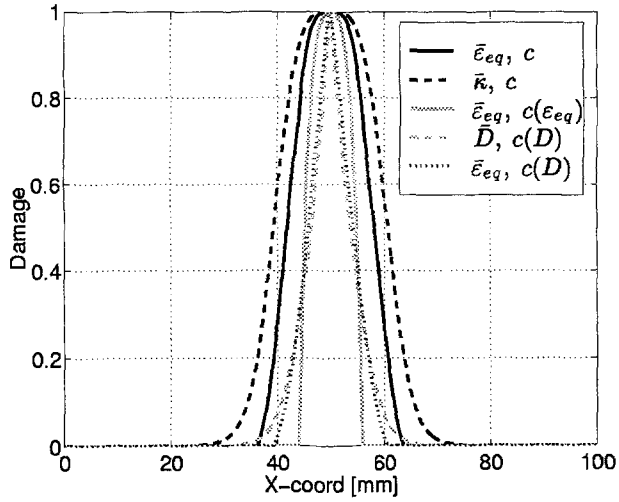

Fig. 8. Damage patterns

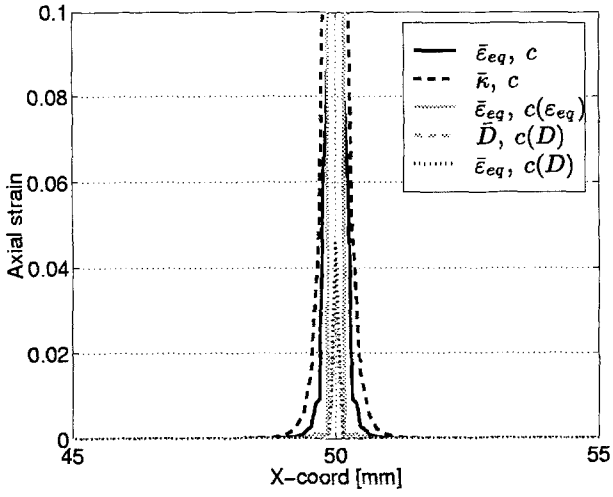

Fig. 9. Strain profiles

stops narrowing for $\bar{\varepsilon}_{eq}$ and $\bar{\kappa}$ as soon as the critical value κ_c is reached, while the narrowing process continues for the $[\bar{\varepsilon}_{eq}, c(\varepsilon_{eq})]$ (17) case. This is illustrated in Fig. 9, where the final strain profiles (in the central 10 mm of the bar) obtained using the power-law damage evolution are depicted for the five models. Both the $[\bar{D}, c(D)]$ and the $[\bar{\varepsilon}_{eq}, c(D)]$ lead to relatively small final strains compared to the three other models. The $[\bar{\varepsilon}_{eq}, c(\varepsilon_{eq})]$ approach gives the most localized response with a peak value (not shown in the Figure) which is approximately 5 times higher than the peak value of the $\bar{\varepsilon}_{eq}$ (7) model, and 17 times higher than the peak strain of the $\bar{\kappa}$ (10) model. Furthermore, it was still possible (at an almost zero stress level) to continue the computation with the $[\bar{\varepsilon}_{eq}, c(\varepsilon_{eq})]$ model, which would then lead to even higher peak values in a progressively smaller zone. Notice that the response of the latter model obtained with an exponential damage evolution law (Fig. 7) hardly differs from the result obtained with the power-law damage evolution (Fig. 8). Analysis of the damage profiles for the exponential damage evolution law showed that no remarkable differences occur (these profiles are therefore not shown), with the exception of the spurious widening which is inevitable with constant c models [12].

5 Crack propagation

Once a crack is initiated, it will propagate through the continuum. Modelling differences with respect to the initiation process were highlighted in the previous section, and the consequences on the propagation stage will now be further examined. To this purpose, a simple, two-dimensional, plane stress, crack propagation example will be analyzed. The specimen for this analysis is depicted in Fig. 10. The length L and the height of the square specimen both equal 60 mm, while the notch length a_n measures 12 mm. The width w_n of the notch equals 7.5 mm, and the specimen thickness t equals 1 mm. The load is applied to the left upper and lower edges of the specimen and is placed at a distance of 4 mm from the left edge. The force-displacement curves, determined at the point where the load is applied, are shown for the five formulations in Fig. 11, where the exponential damage evolution law has been adopted. It is observed that the $\bar{\varepsilon}_{eq}$ (7), the $\bar{\kappa}$ (10) and the $[\bar{\varepsilon}_{eq}, c(\varepsilon_{eq})]$ (17) models give almost identical results. The tail of the load-displacement curve of the transient model is slightly higher, which is in agreement with the one-dimensional results. The $[\bar{D}, c(D)]$ (12) formulation clearly fails to describe the crack propagation process, since it keeps converging to a zero crack opening accompanied by a perfectly brittle crack propagation. The $[\bar{\varepsilon}_{eq}, c(D)]$ (16) approach shows a remarkably different response, which is more brittle than the first three cited models. Snap-back behaviour, which was already observed in the initiation stage, persists but is now followed by an apparently stable softening path. The transition from the unstable snap-back part to the snap-through part of the loading curve is related to the transition from crack initiation to crack growth. A similar analysis can be made for the power-law damage evolution. However, as already mentioned in the crack initiation analysis, the critical damage level $D = 1$ is reached at a finite strain for some models. Since the material has then entirely lost its stiffness, the equilibrium equations locally become meaningless, and the FE formulation may become singular. This singularity may be avoided by introducing a small residual stiffness, but the (nonphysical) deformations in the crack then give rise to a (nonphysical) widening of the damage zone [12]. Such a singularity can also be eliminated through a modification of the mesh (element removal) or of the nodal connectivity (decoupling of nodes). Some form of

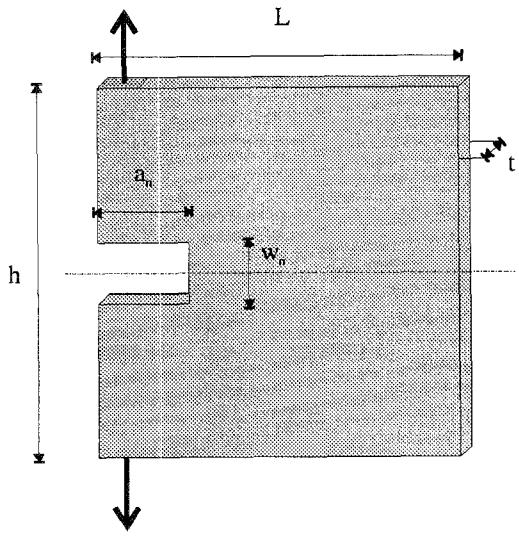

Fig. 10. Two-dimensional test specimen

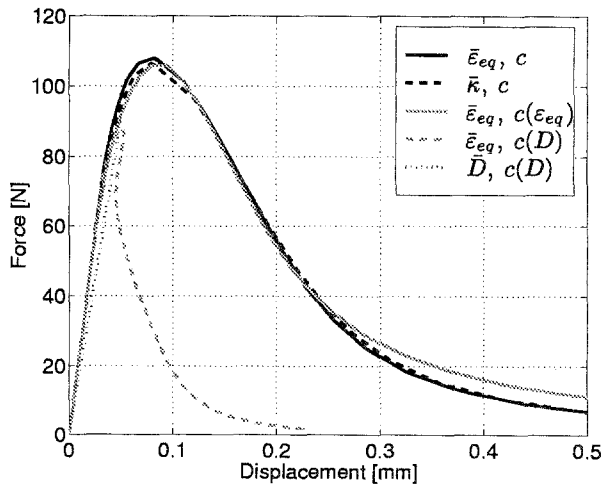

Fig. 11. Global force-displacement curves for the exponential damage evolution

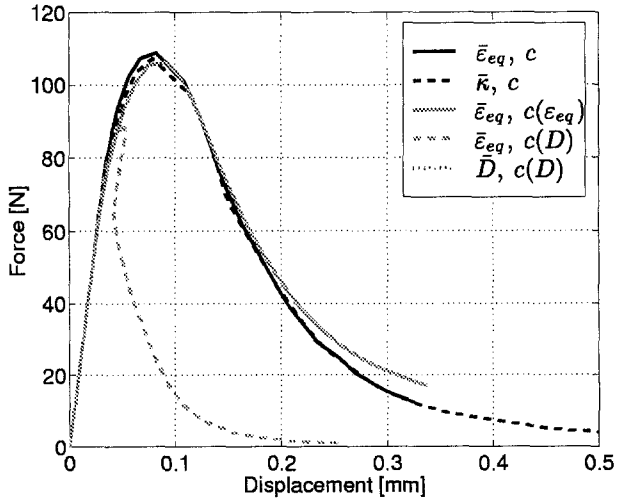

Fig. 12. Global force-displacement curves for the power-law damage evolution

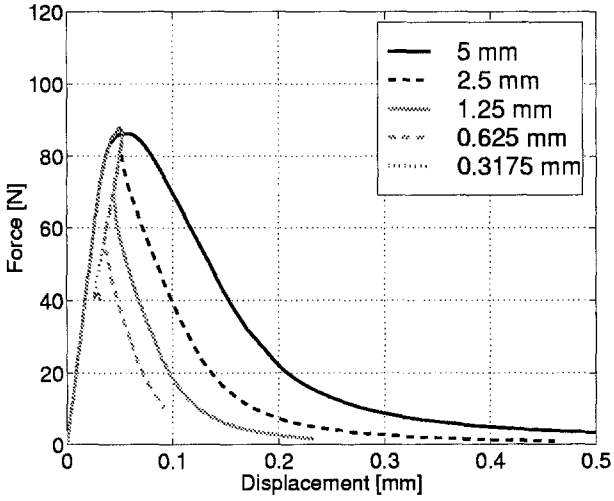

Fig. 13. Convergence of the $\bar{\varepsilon}_{eq}$ model with a damage-dependent length scale upon mesh refinement

mesh adaptation is therefore recommended to continue the computation using the $\bar{\varepsilon}_{eq}$ (7) and the $\bar{\kappa}$ (10) model. Due to the specimen symmetry, only half the specimen is modelled, and the fully damaged nodes along the symmetry-axis are progressively released which enables further damage development and crack propagation. This modification is not necessary for the $[\bar{\varepsilon}_{eq}, c(\varepsilon_{eq})]$ model, since the critical value κ_c is reached at high strain levels only. The results are similar to those obtained with the exponential law. Remarkably, there is almost no difference between the $\bar{\varepsilon}_{eq}$ (7) and the $\bar{\kappa}$ (10) formulations, in spite of the different crack openings found in a one-dimensional initiation analysis. Again, the $[\bar{D}, c(D)]$ (12) model fails, and a doubtful result is obtained with the $[\bar{\varepsilon}_{eq}, c(D)]$ (16) approach. In order to make sure that the obtained results are fully converged, a mesh sensitivity analysis has been performed. Convergence has been achieved for the $\bar{\varepsilon}_{eq}$ model, the $\bar{\kappa}$ model and the $[\bar{\varepsilon}_{eq}, c(\varepsilon_{eq})]$ model. The $[\bar{\varepsilon}_{eq}, c(D)]$, however, now clearly presents an unacceptable behavior. Figure 13 illustrates the convergence of the latter formulation with the use of progressively smaller elements along the axis of symmetry of the specimen. This figure shows that the crack initiation stage tends to converge towards a zero crack opening, as was already observed in the one-dimensional analysis. The propagation phase is postponed and requires a decreasing energy upon mesh refinement, which implies that this phase is again ill-posed and converges to a brittle crack that

moves with an infinite speed. A similar behavior occurs for the $[\bar{D}, c(D)]$ (12) model as shown in Fig. 14, although the influence of the element size appears to be less dramatic in this case. It is clear that transient models, for which the intrinsic length scale diminishes with an increasing damage, do not provide a numerically reliable and a physically meaningful solution for the analysis of crack propagation phenomena. Indeed, infinite crack propagation speeds with zero-energy dissipation are physically non-existing.

The damage profiles in a vertical cross-section taken at 20 mm from the left edge (see Fig. 10) are presented in Fig. 15 and 16 for the exponential and power-law damage evolution laws, respectively. The already reported damage widening [12] using exponential damage evolution laws has led to a damage zone which occupies 2/3 of the specimen height for the $\bar{\varepsilon}_{eq}$ and $\bar{\kappa}$ models (Fig. 15). In the $[\bar{\varepsilon}_{eq}, c(\varepsilon_{eq})]$ model this width remains smaller. The profiles obtained with the power-law damage evolution confirm the results that have been obtained in the one-dimensional crack initiation analysis. Moreover, it should be remarked that two-dimensional analyses with this type of damage evolution for the $\bar{\varepsilon}_{eq}$ and the $\bar{\kappa}$ model are only possible if appropriate mesh adaptation or remeshing techniques are used during the propagation of the crack.

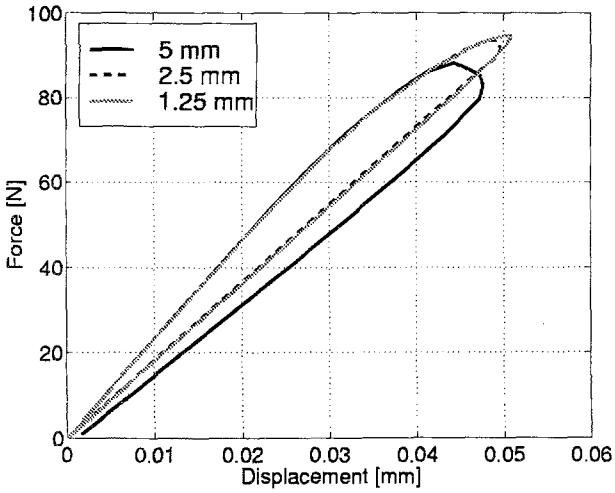

Fig. 14. Convergence of the transient $\bar{D}$ model upon mesh refinement

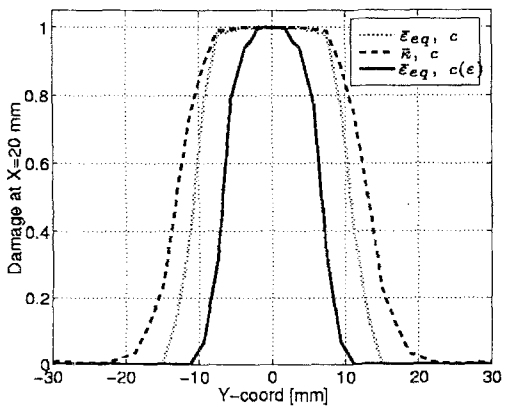

Fig. 15. Exponential

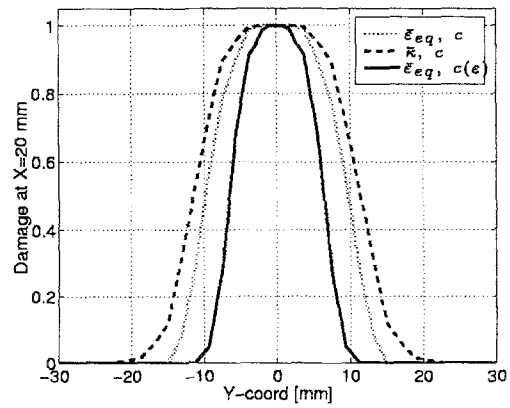

Fig. 16. Power-law

6 Conclusions

Five mutually different implementations of implicit gradient-enhanced damage constitutive models have been examined with respect to their ability to describe crack initiation and crack propagation. The formulations are nonlocal in the sense that an equivalent integral form exists. Three of them contain a variable intrinsic length scale which is either coupled to the damage or to a suitable equivalent strain measure. Two types of damage evolution laws, which resemble well with the exception of the tail of the evolution curve, have been scrutinized, and the results have been discussed. The models were confronted in typical benchmark tests, where the damage evolution laws have been equalized as much as possible.

It has been shown that a model based on a nonlocal equivalent strain with a constant length parameter and a power-law damage evolution leads to a well-defined crack opening in a one-dimensional crack initiation analysis, which can be predicted analytically. Models based on a nonlocal history parameter, a nonlocal damage variable or models with a decreasing length parameter upon increasing damage, systematically yield a zero crack-opening using a power-law damage evolution. If exponential evolution laws are used instead, the nonlocal equivalent strain model and the nonlocal history parameter model, both with a constant length scale, tend to converge to an infinite crack opening. This is typically due to the fact that the crack opening or displacement discontinuity is only approximated in a smooth way. Such a large crack opening is also obtained for a nonlocal equivalent strain model with a length parameter that increases with the strain, but this time the result is less dependent on the type of damage evolution law that has been used. Although one-dimensional results clearly reveal the influence of the tail of the damage evolution curve, this does not necessarily imply that large differences have to be expected in a two-dimensional configuration, where the load is redistributed upon damage evolution.

The analysis of the presented models during crack propagation has revealed the inability of the damage models with a decreasing length parameter upon increasing damage to describe real failure processes. The results indicate that the well-posedness of the problem is again lost after the crack initiation stage, which subsequently leads to a mesh dependent result. The nonlocal equivalent strain model and the nonlocal history parameter model with a constant length scale, and the nonlocal equivalent strain model with a length parameter that increases with the strain, are well capable to describe the crack propagation phenomena. Unless crack openings remain small, the use of exponential damage evolution laws in combination with constant length scales is discouraged. A power-law damage evolution is a versatile alternative, provided appropriate remeshing techniques are used. Nonlocal equivalent strain models with a length parameter that increases with the strain are less sensitive to the type of damage evolution law, and do not require remeshing techniques in the early stage of crack propagation.

Conclusions which are made from one-dimensional analyses may not be extrapolated ad hoc to a two-dimensional problem. It is shown that although the crack initiation may be well-posed, this does not imply that the crack propagation will be so. If the solution at the end of the crack initiation stage approaches the local solution, the damage rate will become singular which leads to a crack that propagates at an infinite speed without any further energy dissipation.

References

[1] Ožbolt, J., Bažant, A. P.: Numerical smeared fracture analysis: nonlocal microcrack interaction approach. Int. J. Numer. Meth. Engng **39,** 635–661 (1996).

[2] Drugan, W. J., Willis, J. R.: A micromechanics-based nonlocal constitutive equation and estimates of representative volume element size for elastic composites. J. Mech. Phys. Solids **44,** 497–524 (1996).

[3] Blechman, I.: Brittle solid under compression. Part I: Gradient mechanisms of microcracking. Int. J. Solids Structures **34,** 2563–2582 (1997).

[4] Tvergaard, V., Needleman, A.: Nonlocal effects on localization in a void-sheet. Int. J. Solids Structures **34,** 2221–2238 (1997).

[5] Eringen, A. C.: A unified theory of thermomechanical materials. Int. J. Engng Sci. **4,** 179–202 (1966).

[6] Maugin, G. A.: Nonlocal theories of gradient-type theories: a matter of convenience? Arch. Mech. **31,** 15–26 (1979).

[7] Delaplace, A., Pijaudier-Cabot, G., Roux, S.: Progressive damage in discrete models and consequences on continuum modelling. J. Mech. Phys. Solids **44,** 99–136 (1996).

[8] Geers, M. G. D., de Borst, R., Brekelmans, W. A. M., Peerlings, R. H. J.: Validation and internal length scale determination for a gradient damage model: Application to short glass-fibre-reinforced polypropylene. Int. J. Solids Sructures **36,** 2557–2583 (1998).

[9] Geers, M. G. D., de Borst, R., Peijs, T.: Mixed numerical-experimental identification of nonlocal characteristics of random fibre reinforced composites. Composites Sci. Technology **59,** 1569–1578 (1999).

[10] Peerlings, R. H. J., Geers, M. G. D., de Borst, R., Brekelmans W. A. M.: A critical comparison of nonlocal and gradient-enhanced continua. Int. J. Solids Structures (forthcoming).

[11] Jirásek, M.: Nonlocal models for damage and fracture: comparison of approaches. Int. Journal Solids Structures **35,** 4133–4145 (1998).

[12] Geers, M. G. D., de Borst, R., Brekelmans, W. A. M., Peerlings, R. H. J: Strain-based transient-gradient damage model for failure analyses. Comp. Meth. Appl. Mech. Engng **160,** 133–154 (1998).

[13] Peerlings, R. H. J., de Borst, R., Brekelmans, W. A. M., de Vree, J. H. P.: Gradient-enhanced damage for quasi-brittle materials. Int. J. Numer. Meth. Engng **39,** 3391–3403 (1996).

[14] de Borst, R., Benallal, A., Heeres, O. M.: A gradient-enhanced damage approach to fracture. J. de Physique IV, **6,** 491–502 (1996).

[15] Geers, M. G. D.: Experimental analysis and computational modelling of damage and fracture. PhD thesis, Eindhoven University of Technology, The Netherlands (1997).

[16] Peerlings, R. H. J., de Borst, R., Brekelmans, W. A. M., Geers, M. G. D.: Gradient-enhanced damage modelling of concrete fracture. Mech. Cohesive-Frictional Mater. **3,** 323–342 (1998).

[17] Geers, M. G. D., de Borst, R., Peerlings, R. H. J.: Damage and crack modelling in single-edge and double-edge notched concrete beams. Eng. Fract. Mech. (forthcoming).

[18] de Borst, R., Geers, M. G. D., Peerlings, R. H. J.: Computational damage mechanics. In: Computational fracture mechanics in concrete technology (Carpenteri, A., Aliabadi, M., eds.), chap. 2, pp. 33–69. WIT Press 1999.

[19] Bažant, Z. P., Pijaudier-Cabot, G.: Nonlocal continuum damage, localization instability and convergence. J. Appl. Mech. **55,** 287–293 (1988).

[20] Frémond, M., Nedjar, B.: Damage, gradient of damage and principle of virtual power. Int. J. Solids Structures **33,** 1083–1103 (1996).

[21] Mühlhaus, H. B., de Borst, R., Sluys, L. J., Pamin, J.: A thermodynamic theory for inhomogeneous damage evolution. In: Computer methods and advances in geomechanics (Siriwardane, H. J., Zaman, M. M., eds.), pp. 635–640. Rotterdam and Boston: Balkema 1994.

Authors' addresses: M. G. D. Geers, R. H. J. Peerlings, W. A. M. Brekelmans, Faculty of Mechanical Engineering, Eindhoven University of Technology, P.O. Box 513, 5600 MB Eindhoven; R. de Borst, Faculty of Aerospace Engineering, Delft University of Technology, The Netherlands; e-mail: geers@wfw.wtb.tue.nl